Article

Cell Reports

Inhibition of Gsk3b Reduces Nfkb1 Signaling and Rescues Synaptic Activity to Improve the Rett Syndrome Phenotype in *Mecp2*-Knockout Mice

Graphical Abstract

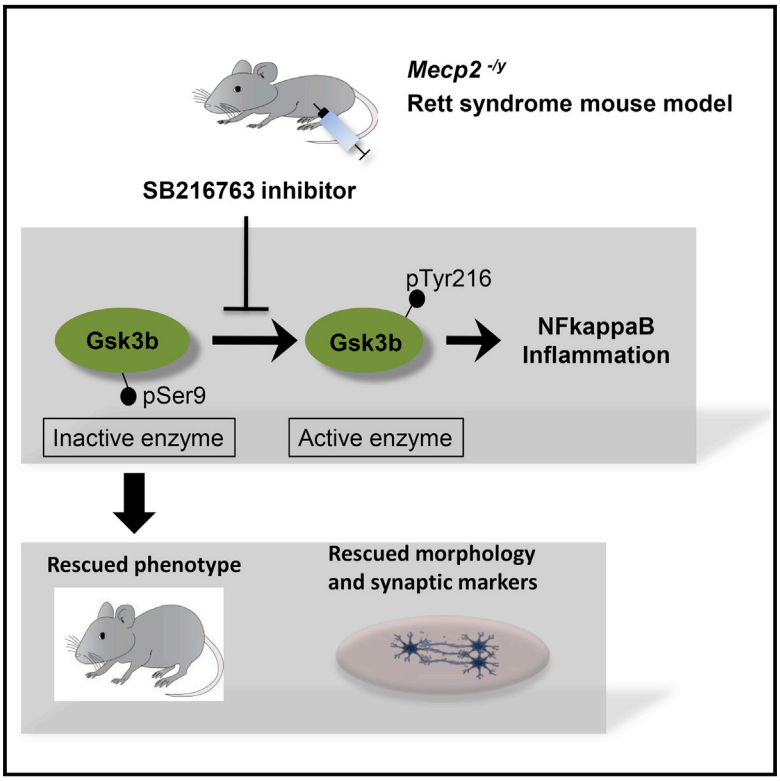

Authors

Olga C. Jorge-Torres, Karolina Szczesna, Laura Roa, ..., Artur Llobet, Sonia Guil, Manel Esteller

Correspondence

sguil@idibell.cat (S.G.),
mesteller@idibell.cat (M.E.)

In Brief

Rett syndrome (RTT) is a severe neurodevelopmental disorder characterized by loss-of-function mutations in the *MeCP2* gene. Jorge-Torres et al. show that mice models of RTT display hyperactivation of Gsk3b kinase and neuroinflammation. Inhibition of the Gsk3b pathway partially rescues the phenotype and affects neuronal morphology and synaptic activity.

Highlights

- Gsk3b kinase activity and inflammation are increased in mice models of Rett syndrome
- Specific inhibition of Gsk3b reduces motor deficits and improves general well-being
- Neuronal morphology is restored *in vitro* and *in vivo* and excitatory synapses altered
- Gsk3b is a potential therapeutic target in Rett syndrome treatment

Jorge-Torres et al., 2018, Cell Reports *23*, 1665–1677
May 8, 2018
https://doi.org/10.1016/j.celrep.2018.04.010

CellPress

Cell Reports
Article

Inhibition of Gsk3b Reduces Nfkb1 Signaling and Rescues Synaptic Activity to Improve the Rett Syndrome Phenotype in *Mecp2*-Knockout Mice

Olga C. Jorge-Torres,[1,11] Karolina Szczesna,[1,11] Laura Roa,[1] Carme Casal,[1] Louisa Gonzalez-Somermeyer,[1] Marta Soler,[1] Cecilia D. Velasco,[2,3,4] Pablo Martínez-San Segundo,[2,3,4] Paolo Petazzi,[1] Mauricio A. Sáez,[1] Raúl Delgado-Morales,[1,5] Stephane Fourcade,[6,7,8] Aurora Pujol,[6,7,8,9] Dori Huertas,[1] Artur Llobet,[2,3,4] Sonia Guil,[1,*] and Manel Esteller[1,9,10,12,*]

[1]Cancer Epigenetics and Biology Program (PEBC), Bellvitge Biomedical Research Institute (IDIBELL), 08908 L'Hospitalet, Barcelona, Catalonia, Spain
[2]Laboratory of Neurobiology, Bellvitge Biomedical Research Institute (IDIBELL), 08907 L'Hospitalet de Llobregat, Barcelona, Catalonia, Spain
[3]Department of Pathology and Experimental Therapeutics, Faculty of Medicine, 08907 L'Hospitalet de Llobregat, Barcelona, Catalonia, Spain
[4]Institute of Neurosciences, University of Barcelona, 08907 L'Hospitalet de Llobregat, Barcelona, Catalonia, Spain
[5]Department of Psychiatry and Neuropsychology, School for Mental Health and Neuroscience (MHeNs), Maastricht University, Maastricht, the Netherlands
[6]Neurometabolic Diseases Laboratory, Bellvitge Biomedical Research Institute (IDIBELL), 08908 L'Hospitalet, Barcelona, Catalonia, Spain
[7]Institute of Neuropathology, University of Barcelona, Barcelona, Catalonia, Spain
[8]Center for Biomedical Research on Rare Diseases (CIBERER), ISCIII, Madrid, Spain
[9]Institucio Catalana de Recerca i Estudis Avançats (ICREA), Barcelona, Catalonia, Spain
[10]Physiological Sciences Department, School of Medicine and Health Sciences, University of Barcelona (UB), 08907 Catalonia, Spain
[11]These authors contributed equally
[12]Lead Contact
*Correspondence: sguil@idibell.cat (S.G.), mesteller@idibell.cat (M.E.)
https://doi.org/10.1016/j.celrep.2018.04.010

SUMMARY

Rett syndrome (RTT) is the second leading cause of mental impairment in girls and is currently untreatable. RTT is caused, in more than 95% of cases, by loss-of-function mutations in the methyl CpG-binding protein 2 gene (*MeCP2*). We propose here a molecular target involved in RTT: the glycogen synthase kinase-3b (Gsk3b) pathway. Gsk3b activity is deregulated in *Mecp2*-knockout (KO) mice models, and SB216763, a specific inhibitor, is able to alleviate the clinical symptoms with consequences at the molecular and cellular levels. *In vivo*, inhibition of Gsk3b prolongs the lifespan of *Mecp2*-KO mice and reduces motor deficits. At the molecular level, SB216763 rescues dendritic networks and spine density, while inducing changes in the properties of excitatory synapses. Gsk3b inhibition can also decrease the nuclear activity of the Nfkb1 pathway and neuroinflammation. Altogether, our findings indicate that Mecp2 deficiency in the RTT mouse model is partially rescued following treatment with SB216763.

INTRODUCTION

Rett syndrome (RTT; OMIM #312750) is a rare neurodevelopmental pathology. It was first described in 1966 as a cognitive impairment disorder affecting 1 in 10,000 female births (Rett, 1966; Hagberg et al., 1983). In 1999, mutations in the *MeCP2* gene were found to be the genetic basis of most cases of RTT (Amir et al., 1999). MeCP2 is a nuclear protein, expressed widely in different tissues but most abundantly in neurons of the mature nervous system, which had been identified a few years earlier by Bird and coworkers as a new protein that bound to the methylated CpG dinucleotides (Lewis et al., 1992).

RTT is an X chromosome-linked, progressive disorder with a normal prenatal and perinatal period. Rett patients have proper brain development during the first few months of age, achieving normal neurodevelopment, motor function, and communication skills. However, developmental regression appears between 8 and 24 months of age (Trevathan and Naidu, 1988; Hagberg, 2002). RTT patients suffer from growth failure, gastrointestinal problems, seizures, and respiratory and cardiac abnormalities. Epilepsy is also one of the main symptoms, with a frequency between 50% and 90% of all cases (Steffenburg et al., 2001; Huppke et al., 2007), although its severity often tends to decrease after adolescence, with lower seizure frequency and fewer secondary generalized seizures (Krajnc et al., 2011).

Because glycogen synthase kinase-3B (GSK3B) has crucial roles in neural development, including neurite growth, specification, and synapse (Seira and Del Río, 2014), we set out to investigate its role in the pathophysiology of RTT. GSK3 is encoded by two genes, *GSK3A* and *GSK3B*, (Frame et al., 2001; Doble and Woodgett, 2003). Both kinases are highly expressed in the brain, but enhanced expression of GSK3B above physiological levels results in hyperactivity and mania (Prickaerts et al., 2006). GSK3 enzymes also have important functions as

regulators of neurotransmitter signaling, as indicated by their control of pathways downstream of dopamine receptors (Beaulieu et al., 2004).

GSK3B is deregulated by tyrosine and serine/threonine phosphorylation; specifically, phosphorylation in Ser9 correlates with the inhibition of its kinase activity (Frame et al., 2001; Wang et al., 1994; Harwood, 2001), while phosphorylation of tyrosine in position 216 is associated with enhanced kinase activity. Several kinases have been reported as targeting the site (Sayas et al., 1999; Hartigan et al., 2001), and even an intramolecular autophosphorylation event has been described (Cole et al., 2004).

Overexpression of a constitutively active GSK3B in cultured neurons reduces expression and clustering of the synaptic protein synapsin I (Zhu et al., 2007), while pharmacological inhibition of GSK3B activity induces synapsin I clustering in developing neurons (Hall et al., 2002). Moreover, activation of GSK3B reduces expression of postsynaptic markers and suppresses release of presynaptic glutamate by inhibiting the synaptic vesicle exocytosis in response to membrane depolarization (Zhu et al., 2010). GSK3B negatively regulates synaptic vesicle fusion events through interference with Ca^{2+}-dependent SNARE complex formation. Other studies have also reported functional roles of GSK3B in the regulation of N-methyl-d-aspartic acid (NMDA) receptor-dependent synaptic plasticity (Decker et al., 2010; Peineau et al., 2008; Li et al., 2009). Activation of GSK3B mediates induction of NMDA-dependent long-term depression (LTD). In contrast, inhibition of GSK3B activity prevents LTD and participates in long-term potentiation (LTP) induction (Hooper et al., 2007). Importantly, an abnormal increase in Gsk3b levels and activity has been associated with neuronal pathologies, and its inhibition has been proposed to be of therapeutic applicability in Alzheimer's disease (Medina and Avila, 2010) and fragile X syndrome (Mines and Jope, 2011). Additionally, GSK3B is involved in inflammation and oxidative damage in the brain, which blocks the production of new neuronal connections in the hippocampus, decreases plasticity and dendritic spine density, and manifests as unsocial behavior. Therefore, drugs that inhibit GSK3B may also prove beneficial in RTT syndrome for controlling cognitive impairments derived from excessive neuroinflammation (Jope et al., 2017).

Mecp2-knockout (KO) mice have a range of physiological and neurological abnormalities that imitate the human syndrome. Here we show that Gsk3b activity is increased in Rett *Mecp2*-KO animals and that by targeting this pathway with a specific inhibitor (SB216763), it is possible to alleviate the symptoms and increase the lifespan of the animals, reduce neuroinflammation markers, and partially restore neuronal connectivity. This makes the Gsk3b signaling pathway an attractive target for therapeutic strategies.

RESULTS

Treatment with the Gsk3b Inhibitor SB216763 Prolongs Lifespan and Ameliorates RTT Symptoms in *Mecp2*-Null Mice

Mecp2- KO mice develop a progression of symptoms in comparison with wild-type (WT) animals. KO mice are globally normal until 4 weeks of age; they then begin to suffer cognitive and motor dysfunctions and fully manifest the RTT-like phenotype at about 6–8 weeks of age (Figure S1A). This leads to rapid weight loss and death at approximately 10 weeks of age (Guy et al., 2001).

To investigate the potential therapeutic role of inhibiting the Gsk3b pathway, three different doses of the specific inhibitor SB216763 were used for the optimization experiment: 0, 0.5, and 1 mg/kg/day. During the whole experiment, none of the selected doses induced a weight loss in the *Mecp2*-KO mice, indicating that the drug was well tolerated and did not have any negative effect on the animals' lifespan in comparison with the vehicle-treated *Mecp2*-KO group. A representative weekly average for a dose of 0.5 mg/kg/day is shown in Figure 1A, which was subsequently used in all experiments and measurements.

After dose optimization, symptom onset was evaluated in the SB216763-treated group compared with the vehicle-treated group. In order to test the effect of the Gsk3b inhibitor SB216763 on the symptoms of RTT mice, behavioral tests were used regularly during the whole treatment procedure. We started treatment when the animals were 4 weeks old, before the onset of disease. The mice were treated daily during 6 weeks and scored twice a week for neurological recovery following previous recommendations (Sutherland et al., 1993). To quantify the alleviation of symptoms after drug administration, we measured mobility, tremor, and breathing features and plotted the average of each phenotypic score during each week of the treatment normalized with the vehicle group (Figures 1B–1D). Treatment with the Gsk3b inhibitor improved the general well-being of the mice; the decrease in scores upon inhibitor treatment corresponded to significant improvements in mobility, tremor, and breathing phenotypes from 7 to 10 weeks of age by an average of 50%–60%, with greater differences appearing at earlier ages. Plotting of the average of the six scored symptoms to create a total score showed a significant phenotypic improvement during the whole time of treatment. SB216763 induced slower progression of the disease, and some of the treated mice did not develop any detectable symptoms until after 8 weeks of age (Figure 1E). The vehicle group displayed an average lifespan of 70 days, whereas in the SB216763-treated group, the average lifespan was 91 days, (Figure 1F; Kaplan-Meier log rank test). Considering the whole population of SB216763-treated mice, the survival curve was 30% longer compared with the vehicle group. Thus, the drug administration in *Mecp2*-KO mice increased their overall well-being by diminishing RTT symptomatology, with no associated intrinsic toxicity, allowing the animals to live longer.

To address in an unbiased manner whether SB216763 administration is associated with reduction of the motor impairments in the *Mecp2*-KO mice, we carried out bar-cross tests. KO mice treated with the drug achieved better scores, suffering fewer slips than vehicle-treated animals (Figures 1G and 1H). Again, the recovery was more noticeable for younger mice. In neophobia or Y-maze tests, we observed not only that the mobility of the KO mice was improved but also that their anxious behavior or susceptibility to stress was reduced (Figures S1B–S1D). We also assessed the effect of starting the treatment at a later time point, from 6 weeks of age, when the symptoms were already present in the animals. As shown in Figures S1E–S1I,

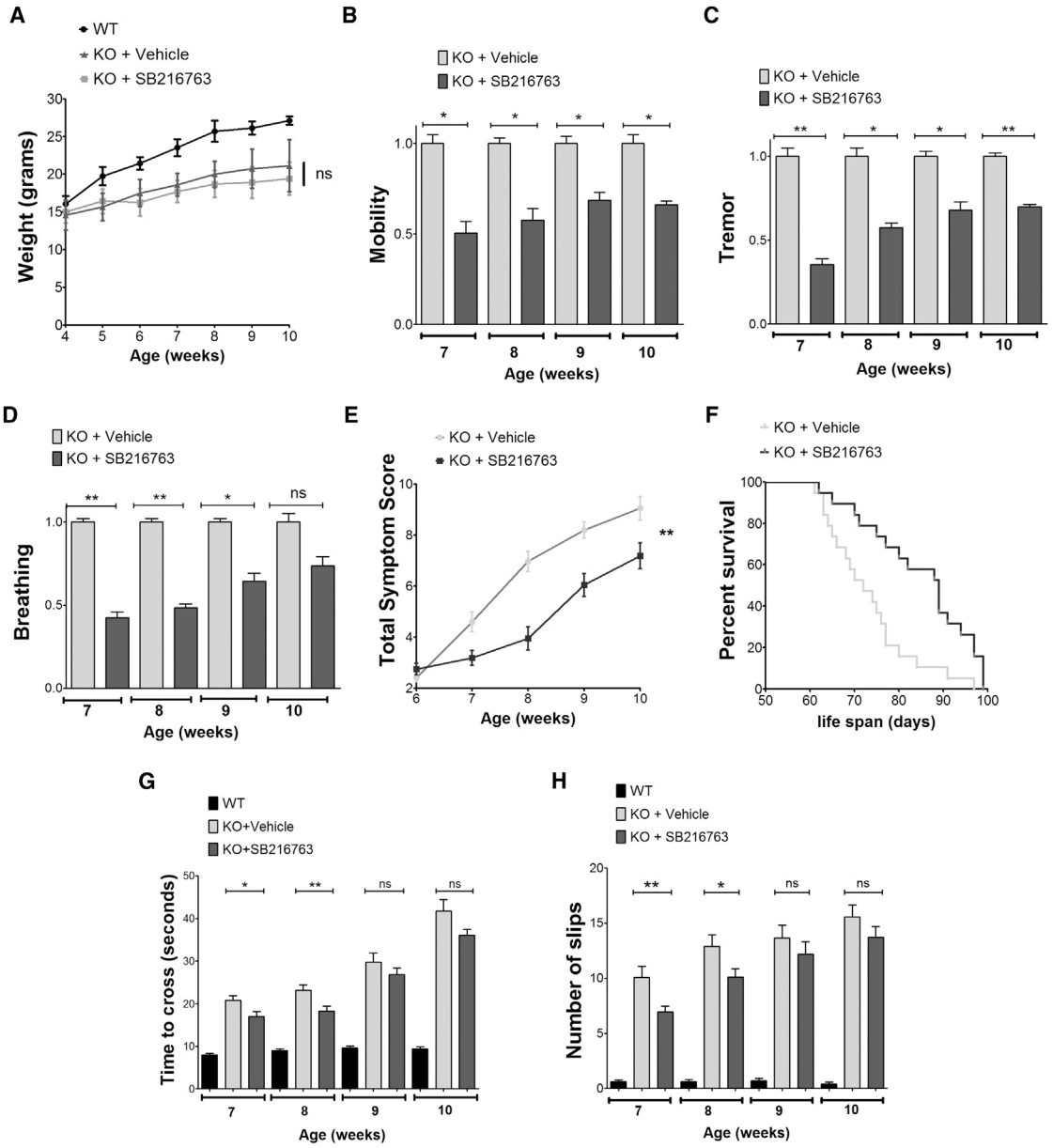

Figure 1. Treatment with the GSK3b Inhibitor SB216763 Ameliorates Symptoms and Prolongs Survival in *Mecp2*-KO Mice

(A) No effect on body weight was observed following drug treatment in KO mice, but KO mice displayed reduced body weight compared with WT animals (n = 10 for both control and treated animals).

(B–D) Bars showing improvement upon SB216763 treatment with respect to mobility (B), tremor (C), and breathing (D) scores (n = 25 for each experimental group).

(E) Representative plot of average total symptom scores. WT mice invariably score 0.

(F) Survival curve using vehicle- and SB216763-treated mice (n = 19 for each group). Log rank test (Mantel-Cox) was used to compare experimental groups, with median survival of 72 days (for control mice) and 89 days (for drug-treated mice).

(G and H) Bar-cross test results show improvement upon treatment with SB216763. The test was carried out once per week; the time spent to cross the bar (G) and number of slips (H) were quantified between the 7th and 10th weeks of age (n = 10 for each group).

Graphs represent mean ± SEM. For the described pairwise comparisons, a Tukey honest significant difference (HSD) post hoc test was performed after one-way ANOVA. *$p < 0.05$ and **$p < 0.01$. See also Figure S1.

drug administration at later times resulted in a slight tendency toward improvement of the phenotype (although not statistically significant).

In view of these results, we went on to characterize changes in the Gsk3b pathway following SB216763 administration at the molecular and cellular level.

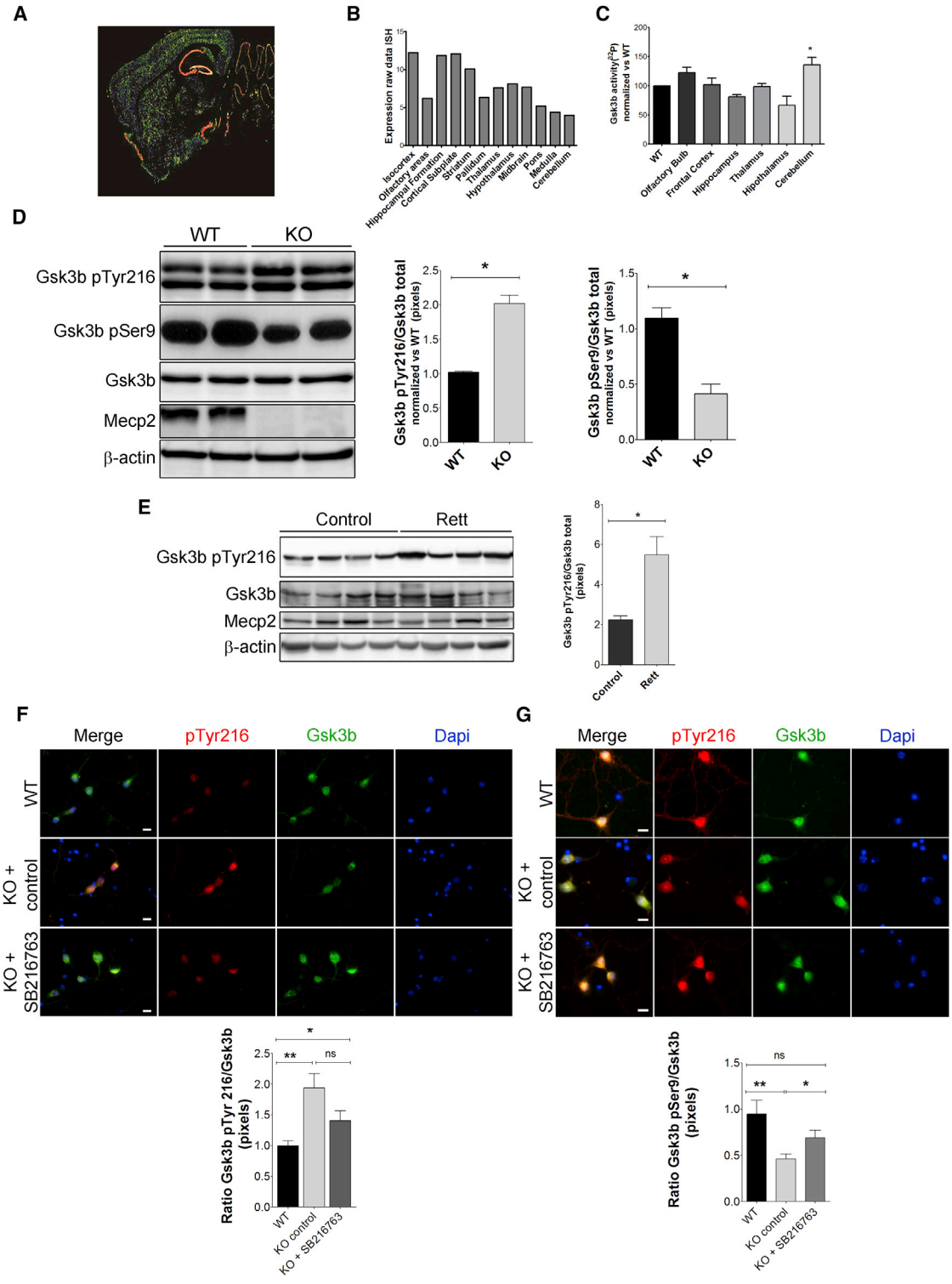

Figure 2. The Kinase Activity of GSK3b Increases in the Cerebellum of 8-Week-Old *Mecp2*$^{-/y}$ Mice

(A and B) Analysis of Gsk3b expression in different mouse brain regions, male P56; sagittal hybridization-ISH (A) and graph displaying raw data (B) are shown. Data are taken from the Allen Institute for Brain Science (available at http://mouse.brain-map.org).

(C) *In vitro* measurement of the kinase activity of Gsk3b from *Mecp2* WT or KO mice brain regions. Graphs represent mean ± SEM; n = 3 per each group.

(D) Representative western blot of total and phosphorylated Gsk3b in cerebellum extracts of WT or *Mecp2*-KO mice. Phosphorylation of residues Tyr216 (indicative of active protein) and Ser9 (indicative of inactive protein) were analyzed. The graphs represent the mean of values ± SEM for WT and KO (n = 2 per group).

(legend continued on next page)

Activity of Gsk3b Is Upregulated in the Cerebellum of Mice Models of RTT and in Human Post-mortem Samples and Can Be Attenuated with SB216763

The Gsk3b protein is ubiquitously distributed in mammalian tissues (Plyte et al., 1992), and its activity is an important component in the regulation of complex functions (Grimes and Jope, 2001). The regulation of Gsk3b can occur through the phosphorylation of specific residues, which may either activate or inactivate the kinase. Inactivation can occur through phosphorylation of serine-9 (Sutherland et al., 1993), serine-389, and threonine-390 (Thornton et al., 2008), or threonine-43 (Ding et al., 2005), while activation can occur through the phosphorylation of tyrosine-216 (Hughes et al., 1993).

Gsk3b mRNA is broadly distributed in normal mouse brain, as shown by *in situ* hybridization (ISH) analysis in sagittal brain tissue of P56 male mice. Regions with the highest signal include the isocortex, the hippocampus, and the striatum (Figures 2A and 2B; mouse Atlas Brain, http://mouse.brain-map.org). Comparison of Gsk3b kinase activity in several brain regions of *Mecp2*-null mice against WT regions showed an abnormal increase in Gsk3b activity, especially in the cerebellum (Figure 2C). Although no changes in total Gsk3b protein level were observed, we detected a ~2-fold increase in the phosphorylation levels of Tyr216 (which correlates with enhanced activity of the protein) and a ~2-fold decrease in the levels of Ser9 phosphorylation (which attenuates activity) (Figure 2D), indicating that Gsk3b activity is dysregulated in the cerebellum of the *Mecp2*$^{-/y}$ mouse model. Other brain regions of the same mice did not show this pattern of activating phosphorylation (Figures S2A and S2B), pointing to a cerebellum-specific upregulation of the Gsk3b pathway. Male RTT mice models recapitulate most of the human symptoms (Lombardi et al., 2015) but are arguably a limited source of knowledge for the understanding of a disorder that affects mainly females. We thus analyzed the levels of phosphorylated Gsk3b in the cerebellum of 8-month-old (fully symptomatic) heterozygous *Mecp2*$^{+/-}$ female mice of the same strain. We also observed an increase in the level of Gsk3b pTyr216 (Figure S2C). Importantly, cerebellar extracts of post-mortem brains from Rett patients displayed the same upregulation (Figure 2E), supporting the idea that aberrant hyperactivation of GSK3 is a hallmark of RTT. Because Akt is one of the main inhibitors of Gsk3b through phosphorylation of Ser9 (Manning and Toker, 2017), these results are in accordance with the dysfunction of the Akt/mTOR signaling pathway reported by others in Rett mice models (Ricciardi et al.,2011). To confirm these observations, we established neuronal primary cultures from either WT or *Mecp2*$^{-/y}$ newborn mouse brains and carried out immunofluorescence staining to detect Gsk3b phosphorylated residues. As shown in Figures 2F and 2G, Gsk3b pTyr216 signal was increased and pSer9 signal was decreased in neuronal cultures derived from the *Mecp2*-null brains, pointing to an enhanced activity of Gsk3b also in these primary cultures. Remarkably, treatment of the cultures with the Gsk3b inhibitor SB216763 partially restored both signals to the levels of the WT neurons, with significant differences between the control-treated and the inhibitor-treated Mecp2$^{-/y}$ neurons.

Inhibition of Gsk3b Reduces Nfkb1 Signaling and Inflammation Levels *In Vivo*

Gsk3b activation has been associated with increases in neuroinflammation and microglial activation, partly by enhancing the nuclear factor kappa b subunit 1 (Nfkb1) pathway (Wang et al., 2010; Hoeflich et al., 2000; Ko et al., 2014). To test whether this is the case in the RTT *Mecp2*-null mice model, we analyzed nuclear Rela/p65 levels (indicative of the functional form as a co-transcriptional regulator) by fluorescence staining in cerebellar neuronal primary cultures. We found that nuclear p65 signaling is upregulated in *Mecp2*-deficient neurons, whereas treatment with SB216763 restored the WT localization (Figure 3A). Total p65 levels were also increased in KO animals and could be downregulated with the inhibitor, as seen *in vivo* by western blot analysis of total brain protein extract from WT and *Mecp2*-KO mice treated with the GSK3b inhibitor (Figure 3B).

Mecp2 depletion can trigger the dysregulation of inflammatory responses and the activation of microglia (which is subsequently lost as the disease progresses) in RTT mice models (Cronk et al., 2015; Derecki et al., 2013). This is in accordance with previous findings describing gliosis and cell loss in the cerebellum of post-mortem RTT brains (Oldfors et al., 1990). In our study, analysis by immunofluorescence of the microglial marker Cd11b showed high infiltration of microglial cells in the cerebellum of 8-week-old *Mecp2*-null mice, which was substantially reduced in mice treated with Gsk3b inhibitor (Figure 3C). Similar results were obtained in the analysis of the pons region next to the cerebellum (Figure S3A). This was confirmed by qRT-PCR that measured the levels of *Cd11b* mRNA (Figure 3D) and of the microglial activator Toll-like receptor 4 (*Tlr4*) (Figure 3E). To get a broader view of the imbalance in inflammatory cell function and of how SB216763 treatment could restore normal levels, we used a commercial antibody array to interrogate 40 mouse cytokines in the cerebellum of *Mecp2*-KO control or KO-treated mice (Figures S3B and S3C). As shown in Figure 3F, inhibition of Gsk3b downregulates a number of pro-inflammatory interleukins, including IL-1α, IL-1β, IL-4, IL-12p70, IL-17, and KC/CXCL1.

(E) Analysis by western blot of cerebellar extracts from post-mortem human brains shows an increase in the levels of active Gsk3b (as indicated by pTyr216 amount) in Rett patients (aged 15–22 years) compared with control healthy samples (n = 4 per group). The graph indicates quantitation of the intensity of the bands relative to total Gsk3b and loading control, representing the mean of values ± SEM.

(F) Immunostaining analyses in cerebellar neuronal primary cultures showed an increase in the levels of Gsk3b pTyr216 (red) in *Mecp2*-KO samples, which tended to decrease after treatment with the inhibitor, whereas the total Gsk3b (green) levels did not change. Graphs represent the median intensity ± SEM of the immunostaining signal in each experimental group.

(G) Levels of Gsk3b pSer9 (red) were decreased in KO neurons but recovered upon drug treatment. Graphs below represent the quantification levels of immunofluorescence ± SEM in all experimental groups.

Scale bars represent 10 μm; n = 15 pictures per condition, corresponding to approximately 30 neurons. For statistical comparison, t test and one-way ANOVA were performed. *p < 0.05 and **p < 0.01. See also Figure S2.

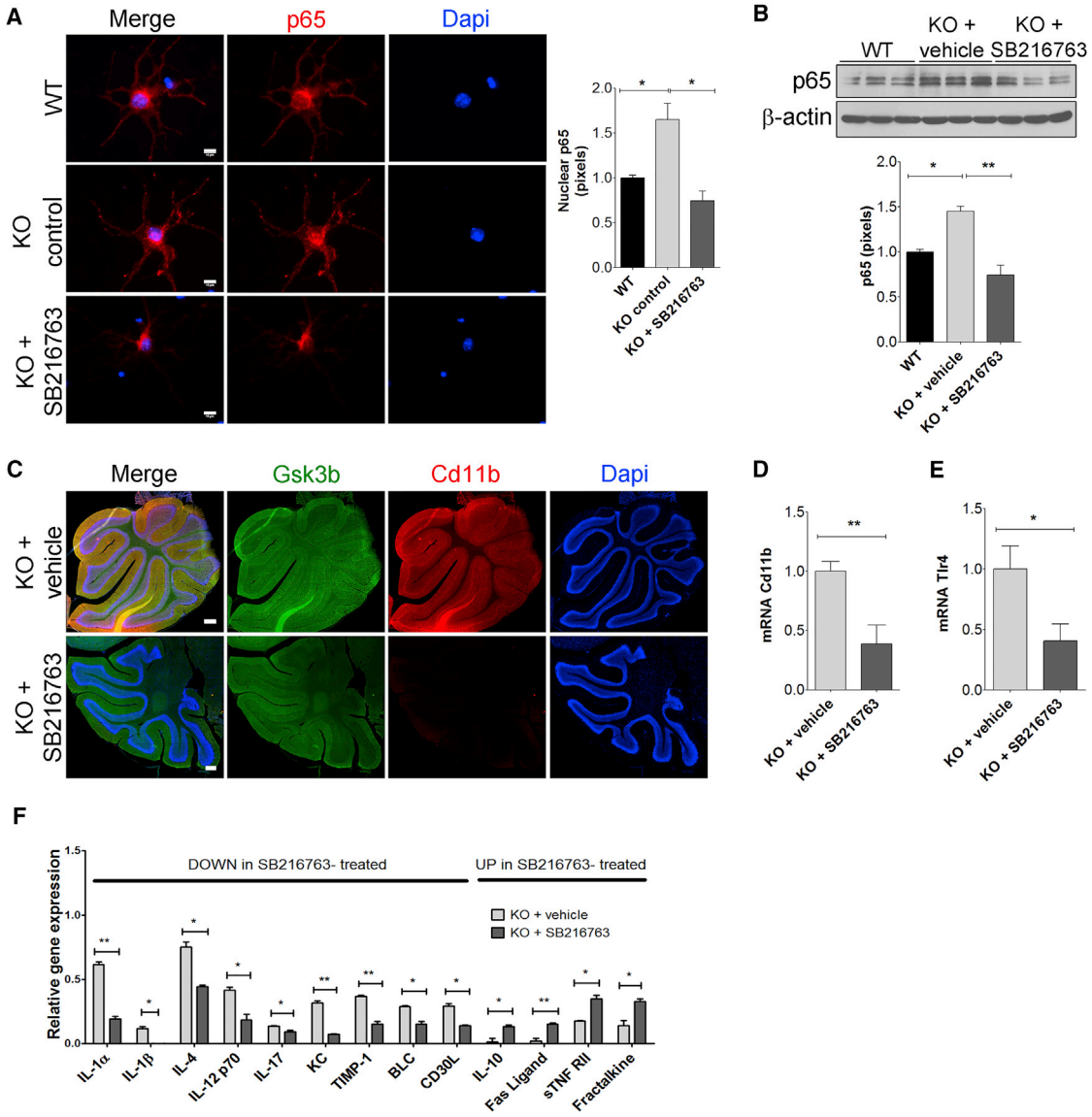

Figure 3. SB216763 Treatment Reduces Inflammation Markers in RTT Model Mice and Primary Neuron Cultures

(A) Nuclear signal of Nfkb1 p65 decreases in KO primary neuron cultures upon treatment with Gsk3b inhibitor. Cells were immunostained with p65 antibody (red) and counterstained with DAPI (blue). Graphs represent the median intensity (pixels) ± SEM of the immunostaining signal in each experimental group. Scale bar represents 10 μm.

(B) Analysis by western blot indicates an increase of p65 levels in *Mecp2*-null total-brain extracts, whereas treatment with the Gsk3b inhibitor restores the WT levels. The graph on the right indicates mean values ± SEM of the three biological replicates.

(C) SB216763-treated cells show attenuation of microglia migration after treatment. Representative immunostaining of Cd11b (microglial marker) in the cerebellum of sagittal sections counterstained with DAPI (blue). All images were processed with ImageJ Fiji version 1.50g. Scale bar represents 100 μm.

(D and E) Expression levels of Cd11b (D) and Tlr4 (E) in cerebellum extracts were determined by qRT-PCR. Mean values ± SEM are represented (n = 3 animals per group).

(F) Comparison of the levels of a panel of cytokines in cerebellar extracts of 8-week-old *Mecp2*-KO control mice and KO-treated mice, as revealed by a cytokine antibody array. Cytokines that went significantly down or up following treatment are indicated. Mean values ± SEM are indicated.

For statistical comparison, t test, one-way ANOVA, and Bonferroni's multiple comparison as post hoc test were performed. *$p < 0.05$ and **$p < 0.01$. See also Figure S3.

Conversely, Fas ligand increases moderately in SB216763-treated animals, which is indicative of the reaction to an excessive immune response. Similarly, the anti-inflammatory cytokine IL-10 is also upregulated upon Gsk3b inhibition. IL-10 is known to block NFKB1 activity and to be involved in the regulation of the JAK-STAT signaling pathway (Mosser and Zhang, 2008).

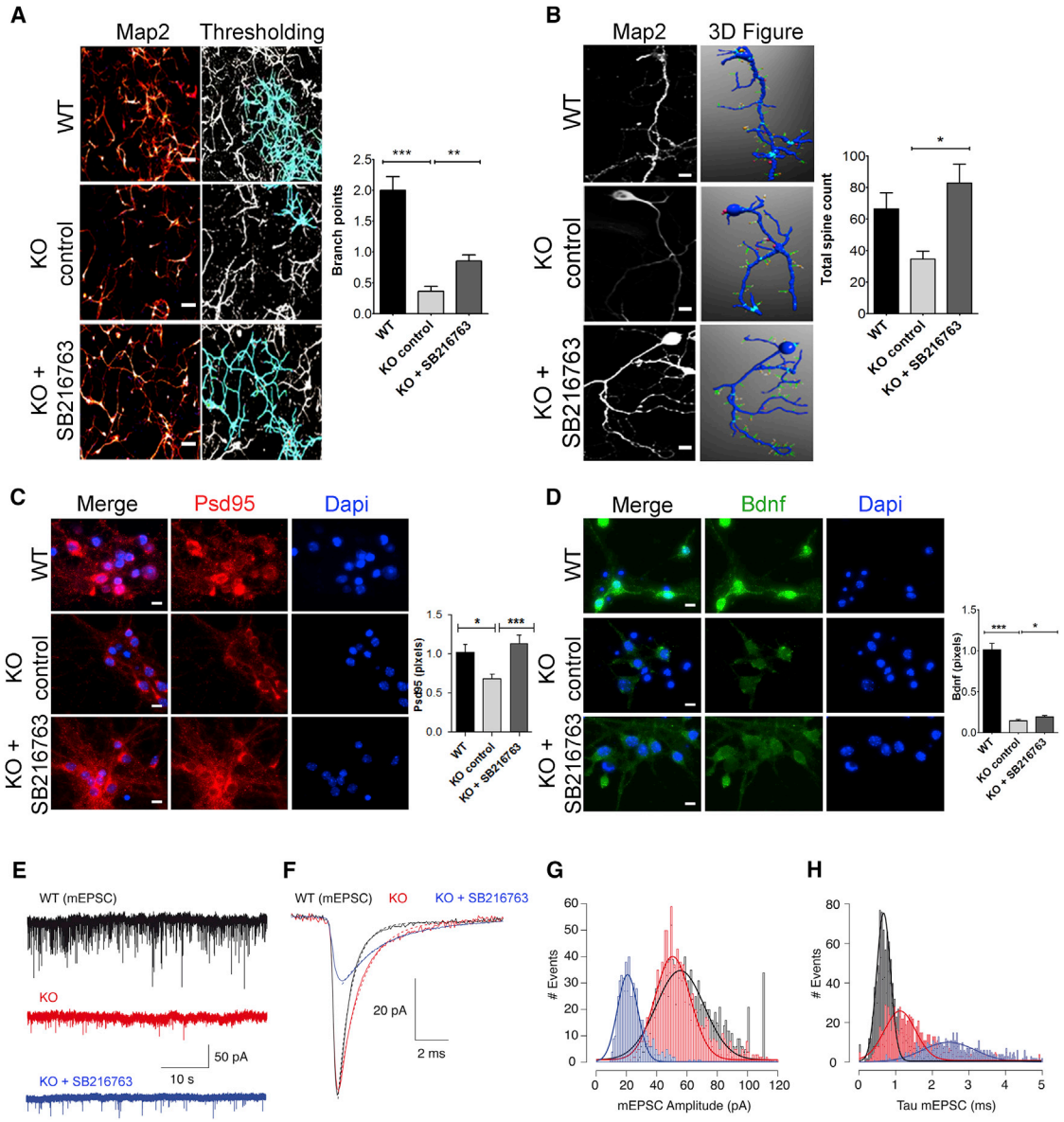

Figure 4. Neuronal Morphology and Synaptic Activity upon *In Vitro* Treatment with the Gsk3b Inhibitor SB216763

(A) Alterations in the complexity of dendritic arborization and connectivity are partially restored with SB216763 treatment. Neurons were immunostained with Map2 (red, left column), and a thresholding analysis with reconstruction of the dendritic network is also shown (right column). Graphs represent the average branchpoints ± SEM. Scale bar represents 50 μm.

(B) Representative analysis of dendritic spine density in WT, control-treated, or SB216763-treated KO primary neurons. Neurons were immunostained with Map2, pictures were obtained with a confocal microscope, and three-dimensional (3D) figures were obtained and analyzed using the Sholl algorithm. raph shows the total spine count (mean ± SEM) in dendritic segments of 20 μm.

(C and D) The levels of Psd95 (C) and Bdnf (D) increase following treatment with the Gsk3b inhibitor. Pictures show representative immunostainings of total brain primary cultures with Psd95 (red) and Bdnf (green) antibodies, counterstained with DAPI (blue). In all experiments, n = 10 pictures per condition, corresponding to 20–30 neurons. Quantification bars represent the integrated density (pixels) of signal using ImageJ Fiji version 1.50g. All data are represented as mean ± SEM. Scale bars represent 10μm. For statistical comparison, one-way ANOVA and Bonferroni's multiple comparison as post hoc test were performed. *$p < 0.05$ and ***$p < 0.001$.

(E–H) Spontaneous excitatory synaptic transmission recorded from cultured cerebellar granule neurons. (E) Miniature excitatory postsynaptic currents (mEPSCs) recorded in primary neurons from WT mice (black) and KO mice (red) appeared at frequencies of ~3 and 0.3 Hz, respectively. Treatment of KO cultures during 48 hr with 0.2 mM SB216763 before recording did not modify mEPSC frequency. (F) Average mEPSCs obtained from three different neurons in the indicated conditions. Notice that mEPSCs are similar in WT and KO cultures, but treatment with 0.2 mM SB216763 decreases the amplitude of spontaneous events. Dotted lines indicate exponential fits to the decay phase of mEPSCs. (G) Distribution of mEPSC amplitudes in the indicated conditions. Solid lines show Gaussian fits for

(legend continued on next page)

In Vitro Treatment with SB216763 Rescues Arborization, Dendritic Spine Density, and Synaptic Activity in Whole-Brain Primary Neuronal Cultures from *Mecp2*$^{-/y}$ Mice

We and others have shown that dendrite branching pattern and density is significantly reduced in mice models and post-mortem brain samples from RTT individuals (Szczesna et al., 2014; Armstrong et al., 1995; Bauman et al., 1995; Chapleau et al., 2009). We thus wanted to test the effect of SB216763 treatment on dendritic arborization and total spine count in neuronal primary cultures. All neuronal branching was fluorescently labeled when neurons reached 7 days in culture (DIV), using a polyclonal antibody against Map2, a neuron-specific protein localized in dendrites and dendritic spines (Morales and Fifkova, 1989). As expected, there were significant differences in the branching pattern and density of dendrites, with WT neurons displaying a wider dendritic field than KO neurons. Treatment of *Mecp2*$^{-/y}$ neurons with SB216763 enabled an important recovery of dendritic arborizations and an improvement in spine density (Figures 4A and 4B).

We next performed a functional evaluation of the impact of these morphological changes by measuring the expression of some neuronal activity markers. Previous studies have described differences in the levels of the postsynaptic density-95 (Psd95) marker and brain-derived neurotrophic factor (Bdnf) between the WT and the *Mecp2*-null RTT mice model, suggesting a loss of synaptic connectivity and plasticity (El-Husseini et al., 2000). Immunofluorescence staining in whole-brain primary cultures showed lower levels of Psd95 in *Mecp2*-null neurons compared with WT cultures. Remarkably, treatment with 0.2 mM SB216763 recovered its expression to levels similar to the WT condition (Figure 4C). We also investigated the levels of Bdnf because it is a main target for Rett therapies and a significant regulator of synaptic transmission and LTP, playing a role in the formation of certain forms of memory (Leal et al., 2014). Of note, signaling by Bdnf induces inhibition of Gsk3b (Mai et al., 2002), raising the possibility that Bdnf deficiency contributes to the higher kinase activity of Gsk3b. As shown in Figure 4D, treatment with the Gsk3b inhibitor moderately recovered the levels of Bdnf in primary cultures, pointing to an involvement of Gsk3b signaling in Bdnf metabolism. To examine synaptic transmission in cerebellar cultures, we recorded spontaneous neurotransmitter release. We did not detect significant differences in inhibitory neurotransmission between WT and *Mecp2*-KO neurons (Figures S4A–S4C), whereas the frequency of miniature excitatory postsynaptic currents (mESPCs) was severely decreased in KO neurons (Figure 4E). This is in agreement with previous observations showing that hippocampal and cortical neurons in *Mecp2*-KO mice display a decreased firing rate caused mainly by alterations in excitatory neurotransmission (Chao et al., 2007; Meng et al., 2016). Although treatment with SB216763 did not lead to an increase in the frequency of spontaneous neurotransmitter release (Figure 4E), there was a noticeable change in the miniature excitatory postsynaptic current (mEPSC) profile following inhibition of Gsk3b, which modified amplitude and decay time (Figures 4F–4H). These observations allow us to speculate with the presence of specific drug-induced alterations in excitatory neurotransmission that could be involved in the partial rescue of the RTT phenotype in this mouse model.

Recovery of Spinogenesis and Synaptic Activity *In Vivo* upon Inhibition of Gsk3b

The beneficial effects of SB216763 on the RTT phenotype was finally tested *in vivo* by measuring dendritic spine formation. Using Golgi staining and the Sholl analysis algorithm (Rodriguez et al., 2008), we found that RTT mice treated with SB216763 showed a significant increase in the number of spines in comparison with vehicle-treated animals (Figure 5A). In accordance with this observation, the expression of the dopamine receptor D2 (Drd2) (which elicits spine formation; Fasano et al., 2013) was increased ~2-fold in the treated animals (Figure 5B), indicating that spinogenesis might be improved through inhibition of the Gsk3b pathway. Neuronal arborization and spine density have a direct link with synaptic activity, thus we next asked whether SB216763 treatment could restore synaptic connectivity. We examined the cell distribution pattern of presynaptic (Vglut1) and postsynaptic (Psd95) markers specific to glutamatergic neurons in WT and *Mecp2*-KO hippocampal tissue of mice brain (Figure 5C). No significant changes were observed at the level of Vglut1 expression, whereas levels of Psd95 were markedly decreased in *Mecp2*-null tissues. Interestingly, treatment with Gsk3b inhibitor partially restored the WT levels, confirming the suitability of Gsk3b pathway inhibition as a means to reverse the defects in synaptic activity present in RTT.

DISCUSSION

In this study we examined *Mecp2*-null mice after treatment with a Gsk3b inhibitor (SB216763) and provided *in vivo* and *in vitro* evidence that the Gsk3β pathway is involved in the phenotype arising from *Mecp2* deficiency. A previous study has shown that targeting Gsk3b in a mouse model of CDKL5 disorder (which is characterized by Rett-like features) ameliorates neuronal developmental defects (Fuchs et al., 2015). In accordance, our data indicate that the phenotype of *Mecp2*-null mice is partially reverted upon selective inhibition of the Gsk3b pathway. Improvement of the motor abilities might be explained by the specific cerebellar hyperactivation of Gsk3b that we have observed in KO mice and Rett patients. Motor impairments affect a patient's quality of life severely, and our results suggest that Gsk3b inhibitors might specifically affect this aspect of the disorder. The best results were observed when treatment started shortly after early development of the phenotype (at 4 weeks of age), and administration starting at later time points showed

each experimental group. mEPSCs recorded after treatment with 0.2 mM SB216763 showed about half the size of control or KO neurons. (H) Distribution of mEPSCs decay times calculated from single exponential fits. mEPSCs recorded after treatment with 0.2 mM SB216763 were longer lasting than in control or KO conditions.
See also Figure S4.

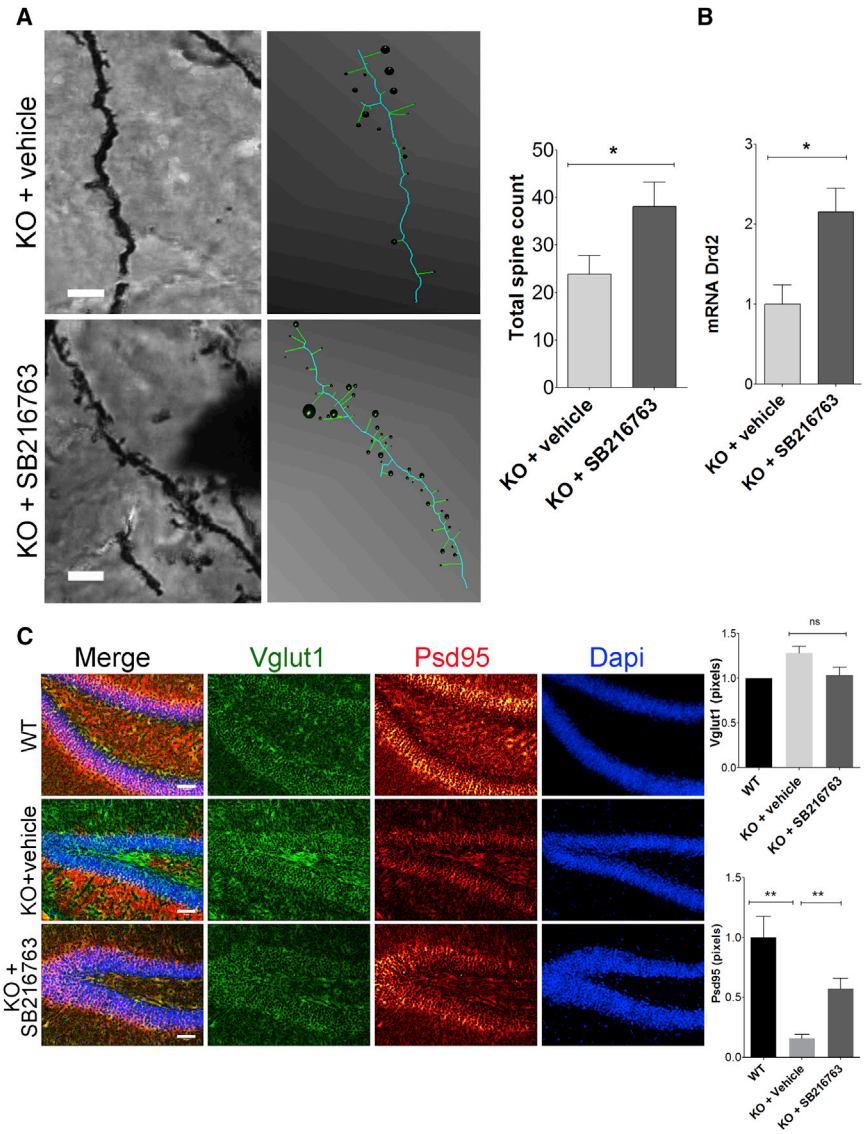

Figure 5. Gsk3b Inhibition Improves Neuronal Morphology and Connectivity *In Vivo*

(A) Changes in dendritic spine density in a brain of *Mecp2*-KO mice 4 weeks post-treatment with Gsk3b inhibitor. Left: a representative picture of dendritic segments in the midbrain region of *Mecp2*-KO mice with or without treatment; right: a 3D reconstruction of tracing dendrites. At least ten neurons were analyzed from two animals per group. Dendritic spine density in segments of 20 μm were analyzed after Golgi staining; the graph shows the average of the total spine count (mean ± SEM) for each condition.

(B) Expression levels of dopamine 2 receptor (Drd2) mRNA in cerebellum, as assessed by qRT-PCR, are increased upon Gsk3b inhibition (graph represents mean values ± SEM, n = 2 per group).

(C) Analysis of neuronal activity markers in the hippocampus of *Mecp2*-KO mice following SB216763 administration. Pictures show a representative staining of Psd95 (postsynaptic marker, in red) and of Vglut1 (presynaptic marker, in green) in the hippocampal region of WT, symptomatic *Mecp2*-KO control mice, and SB216763-treated KO mice (10 weeks old). The graphs represent the integrated density (pixels) of positive signaling using ImageJ Fiji version 1.50g.

All data are mean ± SEM from several replicas. Scale bar represents 50 μm.

weaker beneficial effects, indicating Gsk3b targeting might be optimal at the early stages of the disease.

At the molecular level, we observed an abnormal hyperactivation of Gsk3b in KO mice, which is reverted with the specific inhibitor. These results may explain why previous studies suggest that recombinant human insulin-like growth factor 1 (IGF1) may ameliorate many clinical features of RTT (Khwaja et al., 2014). IGF1 promotes mechanisms that can regulate the inactivation of GSK3β via Ser-9 phosphorylation through direct interaction with AKT (Grimes and Jope, 2001; Shaw et al., 1997; van Weeren et al., 1998).

A downstream target of Gsk3b is the transcription factor Nfkb1. Recent research has shown abnormal activation of Nfkb1 signaling due to loss of Mecp2 regulation on Irak1 (a key component of the Nfkb1 pathway). Restoration of Irak1 WT levels results in improvement of dendritic complexity and extends lifespan of *Mecp2*-deficient mice (Kishi et al., 2016). There is strong evidence suggesting a link between Gsk3b and Nfkb1 activation and an increase in inflammation in mice (Hoeflich et al., 2000). We observed an attenuation of Nfkb1 levels after treatment with Gsk3b inhibitor and a marked decrease in inflammation markers in the cerebellar area. We specifically observed downregulation in IL-1, IL-4, IL-12p70, and IL-17 levels following treatment. Previous studies have also shown increases in IL-4 and IL-17 plasma levels in typical Mecp2-RTT patients and a general shift toward the Th2 subtype of $CD4^+$ T cells (Leoncini et al., 2015). In contrast, in peripheral blood samples of CDKL5-RTT patients, both Th1- and Th2-related cytokines were shown to be increased, revealing a complex dysregulation of the cytokine repertoire in these closely related disorders. In our hands, levels of typical microglial-related cytokines, such as IL-1β, IL-12p70, and IL-10, were also affected by Gsk3b inhibition. Evidence as to the role of microglial function dysregulation in the development of diseases of the central neural system and of RTT in particular is growing, and the restoration of Mecp2 levels in microglial cells has shown positive effects in rescuing the phenotype (Maezawa and Jin, 2010; Lioy et al., 2011; Derecki et al., 2012). These observations, together with the glial infiltration shown in the cerebellar and pons area, reinforce the idea that the pro-inflammatory status has an important role in RTT and that inhibition of Gsk3b activity might reduce the damaging effects of sustained neuroinflammation.

An important finding of our work associated with Gsk3b inhibition is its ability to improve the neuronal dendritic network, supported by spin density measurements and higher levels of Drd2 receptor *in vivo*, placing Gsk3b as a target of potential therapeutic interest to restore the synaptic plasticity deficiencies typical of RTT (Figure S5). In this regard, the activity of Drd2 had already been shown to depend on Gsk3b signaling (L'Episcopo et al., 2012). At the electrophysiological level, we have observed that inhibition of Gsk3b results in marked changes in the signature of excitatory synapses. Targeted reexpression of Mecp2 in glutamatergic neurons has been shown to rescue most of the RTT phenotype in KO mouse models (Meng et al., 2016). Our results thus underscore the relevance of the diminished excitatory signaling in the pathophysiology of RTT and the importance of regulating Gsk3b activity to modulate it. Some analogs of SB216763 have been intensely studied in pre-clinical and clinical assays for their therapeutic value in Parkinson's and Alzheimer's diseases (Lovestone et al., 2015; Poewe et al., 2015). Although the clinical efficacy has not been proved to date, their administration to humans was acceptably safe. Our results expand the potential applicability of such compounds, and we propose that they might represent suitable therapeutic avenues deserving further investigation in the context of RTT.

Overall, the findings reported suggest that the Gsk3b inhibitor SB216763 is able to alleviate the clinical symptoms of the disease with consequences at the molecular and cellular levels in the brain of *Mecp2*-null mouse models. The present work sets the stage for additional research with Gsk3b inhibitors, including dissection of mechanistic details as well as additional pre-clinical testing.

EXPERIMENTAL PROCEDURES

Animals and Pharmacological Treatments

The experiments were performed on the B6.129P2(c)-Mecp2tm1+1Bird mouse model for RTT (Guy et al., 2001). The mice were purchased from Jackson Laboratories (stock number 003890) and maintained on a C57BL/6J background. All the animals were kept under specific pathogen-free conditions with a 12 hr light-dark cycle, with drinking water and food available *ad libitum*. A total of 70 Mecp2$^{-/y}$ (KO null male) and 20 WT mice were used in the study. Unless otherwise stated, treatment with SB216763 began at 4 weeks of age, and mice received daily either an intraperitoneal (i.p.) injection of vehicle (20% DMSO/saline) or SB216763 at a concentration of 0.5 mg/kg (catalog no. S1075, diluted in DMSO 20%; Selleckchem). All procedures and experiments were approved by the Ethics Committee for Animal Experiments of the IDIBELL Centre, under the guidelines of Spanish laws concerning animal welfare. The time points of animal treatment and tissue collection are summarized in Figure S1. Samples from three control or three Mecp2$^{+/-}$ heterozygous female mice of the same strain were taken at 7 months of age, when the symptoms were fully developed.

Score Test

Progression of the RTT phenotype was monitored twice a week following a three-point system (Guy et al., 2001). Neurological defects in KO mice were scored blind to genotype and treatment status, focusing on mobility, gait, hindlimb clasping, tremor, breathing, and general condition. Each of the six symptoms was scored from 0 to 2; 0 corresponds to the symptom's being absent or the same as in the WT, 1 to the symptom's being present, and 2 to the symptom's being severe. The endpoint was reached when the animal score was 2 for each of the three last criteria (tremor, breathing, and general condition). Additionally, if the animal lost 20% of its body weight during the experiment, it was also sacrificed.

Horizontal Bar-Cross Test

The test was carried out as described previously (Ferrer et al., 2005).

Gsk3b Activity Assay

We used the GSK-3β Activity Assay Kit protocol (CS0990; Sigma-Aldrich). Protein extracts from the indicated brain regions were extracted from 8-week-old WT and KO mice using CelLytic M Cell Lysis Reagent (C2978; Sigma-Aldrich). After immunoprecipitation of Gsk3b, kinase activity was assayed by incubation with γ-[^{32}P]-ATP, and ^{32}P incorporation was measured in a Cerenkov counter. Gsk3b activity was expressed as enzymatic activity with substrate minus enzymatic activity without substrate. All values for each region from KO samples were normalized versus the same region in WT samples.

Neuronal Culture

Primary cultures were prepared as described previously (Ahlemeyer and Baumgart-Vogt, 2005). Dissociated cells were seeded at a final density of 7 × 10^5/well (six-well plate) previously coated with poly-D-lysine (1 mg/mL; A003E; Merck). The cell culture was in neurobasal medium (Life Technologies) supplemented with antibiotic (L0022; Biowest), GlutaMAX (35050; Life Technologies), and B27 (2%, supplement for neuronal culture; 17504; Life Technologies). AraC (5 μM cytosine arabinoside; 1768; Sigma) was added to the culture medium 24 hr after plating to limit the growth of non-neuronal cells. The medium was changed every 4–5 days, keeping 50% of the old medium and adding the same volume of fresh medium. After 7 DIV, the neurons were maintained in the same medium and treated with 0.2 mM SB216763. The drugs were maintained in culture during 4 DIV.

Electrophysiology

All experiments were performed in the whole-cell configuration of patch-clamp mode using neurons cultured for 19 DIV. Typical resistances of pipettes used for recordings were ~5 MΩ when filled with internal solution composed of the following: 110 mM CsCl, 4 mM $MgCl_2$, 1 mM EGTA, 10 mM HEPES, 3 mM Na_2ATP, and 1 mM NaGTP (pH 7.2). The external solution contained 130 mM NaCl, 5 mM KCl, 2 mM $CaCl_2$, 1 mM $MgCl_2$, 15 mM glucose, and 15 mM HEPES (pH 7.4). Recordings of mEPSCs were carried out at a holding potential of −70 mV in the presence of 50 μM bicuculine (Tocris) and 1 μM TTX (Tocris). Recordings of spontaneous GABAergic miniature inhibitory postsynaptic currents (mIPSCs) were obtained at −70 mV in the presence of 5 μM CNQX (Tocris) and 1 μM TTX.

All salts were from Sigma-Aldrich. Before the addition of glucose and $CaCl_2$, the osmolality of the external solution was adjusted to 290 mOsm/kg. All experiments were performed at room temperature (23°C). Recordings were made using an Axopatch-1D patch-clamp amplifier (Molecular Devices) under the control of an ITC-18 board (Instrutech) driven by WCP software (Dr. John Dempster, University of Strathclyde). Recordings were acquired at 10 kHz and low-pass-filtered to 5 kHz. Analysis of mEPSCs and mIPSCs was carried out using macros written in Igor Pro software.

Western Blot Cerebellum Total

Western blotting was carried out as previously described (Szczesna et al., 2014). Specific primary antibodies used were Ms-Gsk3b (ab93926; Abcam), Ms-Gsk3b pTyr279/216 (ab75745; Abcam), Rb-mAbGsk3b pSer9 (9323S; Cell Signaling), Rb-CD11b (Ab133357; Abcam), Rb-Mecp2 (PAB0646; Abnova), Rb-Nfkβ P65 (sc-109; Santa Cruz), and β-actin peroxidase conjugated (A3854; Sigma-Aldrich). All antibodies were used at dilutions recommended by the manufacturers and incubated overnight at 4°C in blocking buffer. The quantification of the bands was performed using BIORAD Quantity One version 4.6.5. In all cases, three WT and KO samples were evaluated, although two samples are shown.

Brain post-mortem tissue from control or RTT patients was obtained from the NIH NeuroBioBank at the University of Maryland, Baltimore, and at the Human Brain and Spinal Fluid Resource Center, VA West Los Angeles Healthcare Care Center, Los Angeles, which is sponsored by the National Institute of Neurological Disorders and Stroke (NINDS)/National Institute of Mental Health (NIMH), the National Multiple Sclerosis Society, and the Department of Veterans Affairs.

Cytokine Antibody Array

Semiquantitative analysis of 40 inflammatory factors was performed using the Mouse Inflammation Antibody Array Membrane (ab133999; Abcam). Protein extracts from cerebellar tissue were obtained from 8-week-old *Mecp2*-KO vehicle- or SB216763-treated animals using the 2X Cell Lysis Buffer provided by kit. Protein extract from two mice in each group was pooled into one sample and assayed according to the manufacturer's instructions. Detection of all spots was done using the Amersham Imager 600 imaging system (GE Healthcare), and the integrated density of dots was measured by densitometric analysis with ImageJ software. For each spot, the raw numerical data were extracted and subjected to background subtraction before normalizing the signal for each cytokine to the positive control spots. The results were confirmed by visual comparison of the array images.

Tissue and Primary Neuron Immunofluorescence

Tissue immunostaining was carried out as previously described (Szczesna et al., 2014). The following primary antibodies were used: Ms-Gsk3b (ab93926; Abcam), Rb-Gsk3b pTyr216 (ab75745; Abcam), Rb-mAbGsk3b pSer9 (9323S; Cell Signaling), Rb-Nfkβ p65 (6956; Cell Signaling), Rb-CD11b (Ab133357; Abcam), Ms-Vglut1 (MAB5502; Millipore), Rb-Psd95 (2507; Cell Signaling), and Rb-Bdnf (ab108319; Abcam). Specific secondary antibodies for each condition were used (Alexa Fluor 555 Rb-IgG, A21429, Alexa Fluor 488 Ms-IgG, A21200; Life Technologies). All pictures were obtained using a Zeiss microscope at 40× magnification and processed using ImageJ Fiji version 1.50g. Tile images from sagittal brain sections were obtained at 20× magnification using a Zeiss microscope. Z project and Tile were carried out in order to get complete staining with all antibodies in a larger area. Densitometric analysis was obtained as previously described (Szczesna et al., 2014).

Analysis of Neuronal Morphology "*In Vitro*"

Neuronal primary cultures from WT and KO animals were treated with 0.2 mM SB216763, and the complexity of dendritic arborization and connectivity was analyzed. After 7 DIV, the cell culture was fixed and immunostained with Rb-Map2 antibody (ab5622; Abcam) (following the immunofluorescence staining protocol described above). Pictures and z stacks were obtained using a Zeiss Axio Observer Z1 microscope at 10× magnification with acquisition software ZEN 2011. The images were processed using ImageJ Fiji version 1.50b (http://imagej.nih.gov) using Auto-Threshold (algorithms Mean). Maximum-intensity projection was used for the reconstruction of the three-dimensional dendritic network using NeuronStudio software version 0.9.92. Automated segmentation was obtained with picture thresholding and Sholl analysis taking as a starting point a soma and counting over a length of 20 μm with concentric circles of 10 μm (Sholl, 1953).

Golgi Staining

The study of neuronal morphologies by Golgi staining was done as previously described (Szczesna et al., 2014).

RNA Isolation and Real-Time qPCR Analysis

For total RNA preparation from whole brain or cerebellum, the RNeasy Lipid Tissue Mini Kit (74804; QIAGEN) was used. RNA (2 μg) was retrotranscribed using random hexamers with the ThermoScript RT-PCR System (Invitrogen). Real-time PCR reactions were performed in triplicate on a Roche Lightcycler 480 machine. cDNA (50 ng) was amplified using the SYBR Green PCR Master Mix (Life Technologies) in a final volume of 10 μL. All primer pairs were designed with Primer 3 software and previously validated by gel electrophoresis to amplify specific single products. All data were normalized with the following endogenous controls: Rps28 and β-actin. The following primers were used: *Cd11b* (forward CTGCCTCAGGGATCCGGAAAG, reverse TGTCTGCCTC GGGGATGACATC), *Tlr4* (forward GATTGCTCAAACATGGCAGTTTC, reverse CATTCCAGGTAGGTGTTTCTGCTAA), *Drd2* (forward ATCTCTTGCCCACTGC TCTTTGGA, reverse ATAGACCAGCAGGGTGACGATGAA), Rps28 (forward GGTGACGTGCTCACCCTATT, reverse CCAGAACCCAGCTGCAAGAT), and β-actin (forward GTCGAGTCGCGTCCACC, GTCATCCATGGCGAACTGGT).

Statistical Analysis

Bar graphics and statistical comparisons were obtained using GraphPad Prism version 5.04. Comparative analyses between different experimental groups were performed using unpaired Student's t test and one-way ANOVA with Tukey's or Bonferroni's post hoc test for intergroup comparisons. For the lifespan estimation, data were plotted in Kaplan-Meier survival curves, using the log rank test for survival analysis, plotting survival (Y) as a function of time (X). Results were considered significant if the p value was <0.05, <0.01, or <0.001. Data are expressed as mean ± SEM.

SUPPLEMENTAL INFORMATION

Supplemental Information includes five figures and can be found with this article online at https://doi.org/10.1016/j.celrep.2018.04.010.

ACKNOWLEDGMENTS

We are grateful to all anonymous supporters who contributed to this project through the fund-raising platform Verkami. We thank all staff members in the animal facility at IDIBELL for their excellent technical work. This work was supported by Ministerio de Economía y Competitividad (MINECO) grants SAF2014-56894-R (S.G.) and SAF2015-63568-R (A.L.), Fondation Jérôme Lejeune (M.E.), the Health and Science Departments of the Catalan Government (Generalitat de Catalunya; 2017SGR1080 and 2014SGR633), and the Catalan and Spanish Associations for Rett Syndrome. K.S. was a Dischrom Research Fellow (PITN-GA-2009-238242-DISCHROM, funded by the European Community). S.F. is a Miguel Servet Researcher (CP11/00080, CPII16/00016). A.L. is a Serra Húnter Fellow. A.P. and M.E. are ICREA Research Professors.

AUTHOR CONTRIBUTIONS

All experiments were conceived by O.C.J.-T., K.S., S.G., and M.E. Experiments were carried out mainly by O.C.J.-T. and K.S. L.R. and K.S. carried out the in vivo assays. C.C. provided technical support with microscopic imaging and analysis. L.G.-S. and M.S. helped with maintenance of the mouse colony and brain dissections. S.F. and A.P. helped with the behavioral tests. C.D.V., P.M.-S., and A.L. designed and carried out the electrophysiology recordings. R.D.-M. obtained and analyzed the human samples. O.C.J.-T., L.G.-S., and S.G. developed the GSK3 activity assay. P.P. carried out qRT-PCR analysis. M.A.S. and D.H. designed initial proof-of-concept experiments. O.C.J.-T., S.G., and M.E. wrote the manuscript with the input of all authors. S.G. and M.E. supervised the project.

DECLARATION OF INTERESTS

The authors declare no competing interests.

Received: September 3, 2017
Revised: February 7, 2018
Accepted: March 31, 2018
Published: May 8, 2018

REFERENCES

Ahlemeyer, B., and Baumgart-Vogt, E. (2005). Optimized protocols for the simultaneous preparation of primary neuronal cultures of the neocortex, hippocampus and cerebellum from individual newborn (P0.5) C57Bl/6J mice. J. Neurosci. Methods *149*, 110–120.

Amir, R.E., Van den Veyver, I.B., Wan, M., Tran, C.Q., Francke, U., and Zoghbi, H.Y. (1999). Rett syndrome is caused by mutations in X-linked MECP2, encoding methyl-CpG-binding protein 2. Nat. Genet. *23*, 185–188.

Armstrong, D., Dunn, J.K., Antalffy, B., and Trivedi, R. (1995). Selective dendritic alterations in the cortex of Rett syndrome. J. Neuropathol. Exp. Neurol. *54*, 195–201.

Bauman, M.L., Kemper, T.L., and Arin, D.M. (1995). Pervasive neuroanatomic abnormalities of the brain in three cases of Rett's syndrome. Neurology *45*, 1581–1586.

Beaulieu, J.M., Sotnikova, T.D., Yao, W.D., Kockeritz, L., Woodgett, J.R., Gainetdinov, R.R., and Caron, M.G. (2004). Lithium antagonizes dopamine-dependent behaviors mediated by an AKT/glycogen synthase kinase 3 signaling cascade. Proc. Natl. Acad. Sci. U S A *101*, 5099–5104.

Chao, H.T., Zoghbi, H.Y., and Rosenmund, C. (2007). MeCP2 controls excitatory synaptic strength by regulating glutamatergic synapse number. Neuron *56*, 58–65.

Chapleau, C.A., Calfa, G.D., Lane, M.C., Albertson, A.J., Larimore, J.L., Kudo, S., Armstrong, D.L., Percy, A.K., and Pozzo-Miller, L. (2009). Dendritic spine pathologies in hippocampal pyramidal neurons from Rett syndrome brain and after expression of Rett-associated MECP2 mutations. Neurobiol. Dis. *35*, 219–233.

Cole, A., Frame, S., and Cohen, P. (2004). Further evidence that the tyrosine phosphorylation of glycogen synthase kinase-3 (GSK3) in mammalian cells is an autophosphorylation event. Biochem. J. *377*, 249–255.

Cronk, J.C., Derecki, N.C., Ji, E., Xu, Y., Lampano, A.E., Smirnov, I., Baker, W., Norris, G.T., Marin, I., Coddington, N., et al. (2015). Methyl-CpG binding protein 2 regulates microglia and macrophage gene expression in response to inflammatory stimuli. Immunity *42*, 679–691.

Decker, H., Lo, K.Y., Unger, S.M., Ferreira, S.T., and Silverman, M.A. (2010). Amyloid-beta peptide oligomers disrupt axonal transport through an NMDA receptor-dependent mechanism that is mediated by glycogen synthase kinase 3beta in primary cultured hippocampal neurons. J. Neurosci. *30*, 9166–9171.

Derecki, N.C., Cronk, J.C., Lu, Z., Xu, E., Abbott, S.B., Guyenet, P.G., and Kipnis, J. (2012). Wild-type microglia arrest pathology in a mouse model of Rett syndrome. Nature *484*, 105–109.

Derecki, N.C., Cronk, J.C., and Kipnis, J. (2013). The role of microglia in brain maintenance: implications for Rett syndrome. Trends Immunol. *34*, 144–150.

Ding, Q., Xia, W., Liu, J.C., Yang, J.Y., Lee, D.F., Xia, J., Bartholomeusz, G., Li, Y., Pan, Y., Li, Z., et al. (2005). Erk associates with and primes GSK-3beta for its inactivation resulting in upregulation of beta-catenin. Mol. Cell *19*, 159–170.

Doble, B.W., and Woodgett, J.R. (2003). GSK-3: tricks of the trade for a multitasking kinase. J. Cell Sci. *116*, 1175–1186.

El-Husseini, A.E., Schnell, E., Chetkovich, D.M., Nicoll, R.A., and Bredt, D.S. (2000). PSD-95 involvement in maturation of excitatory synapses. Science *290*, 1364–1368.

Fasano, C., Bourque, M.J., Lapointe, G., Leo, D., Thibault, D., Haber, M., Kortleven, C., Desgroseillers, L., Murai, K.K., and Trudeau, L.É. (2013). Dopamine facilitates dendritic spine formation by cultured striatal medium spiny neurons through both D1 and D2 dopamine receptors. Neuropharmacology *67*, 432–443.

Ferrer, I., Kapfhammer, J.P., Hindelang, C., Kemp, S., Troffer-Charlier, N., Broccoli, V., Callyzot, N., Mooyer, P., Selhorst, J., Vreken, P., et al. (2005). Inactivation of the peroxisomal ABCD2 transporter in the mouse leads to late-onset ataxia involving mitochondria, Golgi and endoplasmic reticulum damage. Hum. Mol. Genet. *14*, 3565–3577.

Frame, S., Cohen, P., and Biondi, R.M. (2001). A common phosphate binding site explains the unique substrate specificity of GSK3 and its inactivation by phosphorylation. Mol. Cell *7*, 1321–1327.

Fuchs, C., Rimondini, R., Viggiano, R., Trazzi, S., De Franceschi, M., Bartesaghi, R., and Ciani, E. (2015). Inhibition of GSK3β rescues hippocampal development and learning in a mouse model of CDKL5 disorder. Neurobiol. Dis. *82*, 298–310.

Grimes, C.A., and Jope, R.S. (2001). The multifaceted roles of glycogen synthase kinase 3beta in cellular signaling. Prog. Neurobiol. *65*, 391–426.

Guy, J., Hendrich, B., Holmes, M., Martin, J.E., and Bird, A. (2001). A mouse Mecp2-null mutation causes neurological symptoms that mimic Rett syndrome. Nat. Genet. *27*, 322–326.

Hagberg, B. (2002). Clinical manifestations and stages of Rett syndrome. Ment. Retard. Dev. Disabil. Res. Rev. *8*, 61–65.

Hagberg, B., Aicardi, J., Dias, K., and Ramos, O. (1983). A progressive syndrome of autism, dementia, ataxia, and loss of purposeful hand use in girls: Rett's syndrome: report of 35 cases. Ann. Neurol. *14*, 471–479.

Hall, A.C., Brennan, A., Goold, R.G., Cleverley, K., Lucas, F.R., Gordon-Weeks, P.R., and Salinas, P.C. (2002). Valproate regulates GSK-3-mediated axonal remodeling and synapsin I clustering in developing neurons. Mol. Cell. Neurosci. *20*, 257–270.

Hartigan, J.A., Xiong, W.C., and Johnson, G.V. (2001). Glycogen synthase kinase 3beta is tyrosine phosphorylated by PYK2. Biochem. Biophys. Res. Commun. *284*, 485–489.

Harwood, A.J. (2001). Regulation of GSK-3: a cellular multiprocessor. Cell *105*, 821–824.

Hoeflich, K.P., Luo, J., Rubie, E.A., Tsao, M.S., Jin, O., and Woodgett, J.R. (2000). Requirement for glycogen synthase kinase-3beta in cell survival and NF-kappaB activation. Nature *406*, 86–90.

Hooper, C., Markevich, V., Plattner, F., Killick, R., Schofield, E., Engel, T., Hernandez, F., Anderton, B., Rosenblum, K., Bliss, T., et al. (2007). Glycogen synthase kinase-3 inhibition is integral to long-term potentiation. Eur. J. Neurosci. *25*, 81–86.

Hughes, K., Nikolakaki, E., Plyte, S.E., Totty, N.F., and Woodgett, J.R. (1993). Modulation of the glycogen synthase kinase-3 family by tyrosine phosphorylation. EMBO J. *12*, 803–808.

Huppke, P., Köhler, K., Brockmann, K., Stettner, G.M., and Gärtner, J. (2007). Treatment of epilepsy in Rett syndrome. Eur. J. Paediatr. Neurol. *11*, 10–16.

Jope, R.S., Cheng, Y., Lowell, J.A., Worthen, R.J., Sitbon, Y.H., and Beurel, E. (2017). Stressed and Inflamed, Can GSK3 Be Blamed? Trends Biochem. Sci. *42*, 180–192.

Khwaja, O.S., Ho, E., Barnes, K.V., O'Leary, H.M., Pereira, L.M., Finkelstein, Y., Nelson, C.A., 3rd, Vogel-Farley, V., DeGregorio, G., Holm, I.A., et al. (2014). Safety, pharmacokinetics, and preliminary assessment of efficacy of mecasermin (recombinant human IGF-1) for the treatment of Rett syndrome. Proc. Natl. Acad. Sci. U S A *111*, 4596–4601.

Kishi, N., MacDonald, J.L., Ye, J., Molyneaux, B.J., Azim, E., and Macklis, J.D. (2016). Reduction of aberrant NF-κB signalling ameliorates Rett syndrome phenotypes in Mecp2-null mice. Nat. Commun. *7*, 10520.

Ko, C.Y., Wang, W.L., Wang, S.M., Chu, Y.Y., Chang, W.C., and Wang, J.M. (2014). Glycogen synthase kinase-3β-mediated CCAAT/enhancer-binding protein delta phosphorylation in astrocytes promotes migration and activation of microglia/macrophages. Neurobiol. Aging *35*, 24–34.

Krajnc, N., Župančič, N., and Oražem, J. (2011). Epilepsy treatment in Rett syndrome. J. Child Neurol. *26*, 1429–1433.

L'Episcopo, F., Tirolo, C., Testa, N., Caniglia, S., Morale, M.C., Deleidi, M., Serapide, M.F., Pluchino, S., and Marchetti, B. (2012). Plasticity of subventricular zone neuroprogenitors in MPTP (1-methyl-4-phenyl-1,2,3,6-tetrahydropyridine) mouse model of Parkinson's disease involves cross talk between inflammatory and Wnt/β-catenin signaling pathways: functional consequences for neuroprotection and repair. J. Neurosci. *32*, 2062–2085.

Leal, G., Comprido, D., and Duarte, C.B. (2014). BDNF-induced local protein synthesis and synaptic plasticity. Neuropharmacology *76*, 639–656.

Leoncini, S., De Felice, C., Signorini, C., Zollo, G., Cortelazzo, A., Durand, T., Galano, J.-M., Guerranti, R., Rossi, M., Ciccoli, L., and Hayek, J. (2015). Cytokine dysregulation in MECP2- and CDKL5-related Rett syndrome: relationships with aberrant redox homeostasis, inflammation, and ω-3 PUFAs. Oxid. Med. Cell. Longev. *2015*, 421624.

Lewis, J.D., Meehan, R.R., Henzel, W.J., Maurer-Fogy, I., Jeppesen, P., Klein, F., and Bird, A. (1992). Purification, sequence, and cellular localization of a novel chromosomal protein that binds to methylated DNA. Cell *69*, 905–914.

Li, Y.C., Xi, D., Roman, J., Huang, Y.Q., and Gao, W.J. (2009). Activation of glycogen synthase kinase-3 beta is required for hyperdopamine and D2 receptor-mediated inhibition of synaptic NMDA receptor function in the rat prefrontal cortex. J. Neurosci. *29*, 15551–15563.

Lioy, D.T., Garg, S.K., Monaghan, C.E., Raber, J., Foust, K.D., Kaspar, B.K., Hirrlinger, P.G., Kirchhoff, F., Bissonnette, J.M., Ballas, N., and Mandel, G. (2011). A role for glia in the progression of Rett's syndrome. Nature *475*, 497–500.

Lombardi, L.M., Baker, S.A., and Zoghbi, H.Y. (2015). *MECP2* disorders: from the clinic to mice and back. J. Clin. Invest. *125*, 2914–2923.

Lovestone, S., Boada, M., Dubois, B., Hüll, M., Rinne, J.O., Huppertz, H.J., Calero, M., Andrés, M.V., Gómez-Carrillo, B., León, T., and del Ser, T.; ARGO investigators (2015). A phase II trial of tideglusib in Alzheimer's disease. J. Alzheimers Dis. *45*, 75–88.

Maezawa, I., and Jin, L.W. (2010). Rett syndrome microglia damage dendrites and synapses by the elevated release of glutamate. J. Neurosci. *30*, 5346–5356.

Mai, L., Jope, R.S., and Li, X. (2002). BDNF-mediated signal transduction is modulated by GSK3beta and mood stabilizing agents. J. Neurochem. *82*, 75–83.

Manning, B.D., and Toker, A. (2017). AKT/PKB signaling: navigating the network. Cell *169*, 381–405.

Medina, M., and Avila, J. (2010). Glycogen synthase kinase-3 (GSK-3) inhibitors for the treatment of Alzheimer's disease. Curr. Pharm. Des. *16*, 2790–2798.

Meng, X., Wang, W., Lu, H., He, L.J., Chen, W., Chao, E.S., Fiorotto, M.L., Tang, B., Herrera, J.A., Seymour, M.L., et al. (2016). Manipulations of MeCP2 in glutamatergic neurons highlight their contributions to Rett and other neurological disorders. eLife *5*, e14199.

Mines, M.A., and Jope, R.S. (2011). Glycogen synthase kinase-3: a promising therapeutic target for fragile x syndrome. Front. Mol. Neurosci. *4*, 35.

Morales, M., and Fifkova, E. (1989). Distribution of MAP2 in dendritic spines and its colocalization with actin. An immunogold electron-microscope study. Cell Tissue Res. *256*, 447–456.

Mosser, D.M., and Zhang, X. (2008). Interleukin-10: new perspectives on an old cytokine. Immunol. Rev. *226*, 205–218.

Oldfors, A., Sourander, P., Armstrong, D.L., Percy, A.K., Witt-Engerström, I., and Hagberg, B.A. (1990). Rett syndrome: cerebellar pathology. Pediatr. Neurol. *6*, 310–314.

Peineau, S., Bradley, C., Taghibiglou, C., Doherty, A., Bortolotto, Z.A., Wang, Y.T., and Collingridge, G.L. (2008). The role of GSK-3 in synaptic plasticity. Br. J. Pharmacol. *153* (*Suppl*), S428–S437.

Plyte, S.E.K., Hughes, K., Nikolakaki, E., Pulverer, B.J., and Woodgett, J.R. (1992). Glycogen synthase kinase-3: functions in oncogenesis and development. Biochim. Biophys. Acta *1114*, 147–162.

Poewe, W., Mahlknecht, P., and Krismer, F. (2015). Therapeutic advances in multiple system atrophy and progressive supranuclear palsy. Mov. Disord. *30*, 1528–1538.

Prickaerts, J., Moechars, D., Cryns, K., Lenaerts, I., van Craenendonck, H., Goris, I., Daneels, G., Bouwknecht, J.A., and Steckler, T. (2006). Transgenic mice overexpressing glycogen synthase kinase 3beta: a putative model of hyperactivity and mania. J. Neurosci. *26*, 9022–9029.

Rett, A. (1966). [On a unusual brain atrophy syndrome in hyperammonemia in childhood]. Wien. Med. Wochenschr. *116*, 723–726.

Ricciardi, S., Boggio, E.M., Grosso, S., Lonetti, G., Forlani, G., Stefanelli, G., Calcagno, E., Morello, N., Landsberger, N., Biffo, S., et al. (2011). Reduced AKT/mTOR signaling and protein synthesis dysregulation in a Rett syndrome animal model. Hum. Mol. Genet. *20*, 1182–1196.

Rodriguez, A., Ehlenberger, D.B., Dickstein, D.L., Hof, P.R., and Wearne, S.L. (2008). Automated three-dimensional detection and shape classification of dendritic spines from fluorescence microscopy images. PLoS ONE *3*, e1997.

Sayas, C.L., Moreno-Flores, M.T., Avila, J., and Wandosell, F. (1999). The neurite retraction induced by lysophosphatidic acid increases Alzheimer's disease-like Tau phosphorylation. J. Biol. Chem. *274*, 37046–37052.

Seira, O., and Del Río, J.A. (2014). Glycogen synthase kinase 3 beta (GSK3β) at the tip of neuronal development and regeneration. Mol. Neurobiol. *49*, 931–944.

Shaw, M., Cohen, P., and Alessi, D.R. (1997). Further evidence that the inhibition of glycogen synthase kinase-3beta by IGF-1 is mediated by PDK1/PKB-induced phosphorylation of Ser-9 and not by dephosphorylation of Tyr-216. FEBS Lett. *416*, 307–311.

Sholl, D.A. (1953). Dendritic organization in the neurons of the visual and motor cortices of the cat. J. Anat. *87*, 387–406.

Steffenburg, U., Hagberg, G., and Hagberg, B. (2001). Epilepsy in a representative series of Rett syndrome. Acta Paediatr. *90*, 34–39.

Sutherland, C., Leighton, I.A., and Cohen, P. (1993). Inactivation of glycogen synthase kinase-3 beta by phosphorylation: new kinase connections in insulin and growth-factor signalling. Biochem. J. *296*, 15–19.

Szczesna, K., de la Caridad, O., Petazzi, P., Soler, M., Roa, L., Saez, M.A., Fourcade, S., Pujol, A., Artuch-Iriberri, R., Molero-Luis, M., et al. (2014). Improvement of the Rett syndrome phenotype in a MeCP2 mouse model upon treatment with levodopa and a dopa-decarboxylase inhibitor. Neuropsychopharmacology *39*, 2846–2856.

Thornton, T.M., Pedraza-Alva, G., Deng, B., Wood, C.D., Aronshtam, A., Clements, J.L., Sabio, G., Davis, R.J., Matthews, D.E., Doble, B., and Rincon, M. (2008). Phosphorylation by p38 MAPK as an alternative pathway for GSK3beta inactivation. Science *320*, 667–670.

Trevathan, E., and Naidu, S. (1988). The clinical recognition and differential diagnosis of Rett syndrome. J. Child Neurol. *3* (*Suppl*), S6–S16.

van Weeren, P.C., de Bruyn, K.M., de Vries-Smits, A.M., van Lint, J., and Burgering, B.M. (1998). Essential role for protein kinase B (PKB) in insulin-induced glycogen synthase kinase 3 inactivation. Characterization of dominant-negative mutant of PKB. J. Biol. Chem. *273*, 13150–13156.

Wang, Q.M., Fiol, C.J., DePaoli-Roach, A.A., and Roach, P.J. (1994). Glycogen synthase kinase-3 beta is a dual specificity kinase differentially regulated by tyrosine and serine/threonine phosphorylation. J. Biol. Chem. *269*, 14566–14574.

Wang, M.J., Huang, H.Y., Chen, W.F., Chang, H.F., and Kuo, J.S. (2010). Glycogen synthase kinase-3β inactivation inhibits tumor necrosis factor-α production in microglia by modulating nuclear factor κB and MLK3/JNK signaling cascades. J. Neuroinflammation *7*, 99.

Zhu, L.Q., Wang, S.H., Liu, D., Yin, Y.Y., Tian, Q., Wang, X.C., Wang, Q., Chen, J.G., and Wang, J.Z. (2007). Activation of glycogen synthase kinase-3 inhibits long-term potentiation with synapse-associated impairments. J. Neurosci. *27*, 12211–12220.

Zhu, L.Q., Liu, D., Hu, J., Cheng, J., Wang, S.H., Wang, Q., Wang, F., Chen, J.G., and Wang, J.Z. (2010). GSK-3 beta inhibits presynaptic vesicle exocytosis by phosphorylating P/Q-type calcium channel and interrupting SNARE complex formation. J. Neurosci. *30*, 3624–3633.